Review of Scientific Instruments

RESEARCH ARTICLE | JANUARY 25 2024

Achromatic, planar Fresnel-reflector for a single-beam magneto-optical trap

S. A. Bondza ; T. Leopold ; R. Schwarz ; C. Lisdat

Rev. Sci. Instrum. 95, 013202 (2024)
https://doi.org/10.1063/5.0174674

AIP Publishing

Review of Scientific Instruments ARTICLE pubs.aip.org/aip/rsi

Achromatic, planar Fresnel-reflector for a single-beam magneto-optical trap

Cite as: Rev. Sci. Instrum. 95, 013202 (2024); doi: 10.1063/5.0174674
Submitted: 1 September 2023 • Accepted: 19 December 2023 •
Published Online: 25 January 2024

S. A. Bondza,[1,2] T. Leopold,[1,2] R. Schwarz,[2] and C. Lisdat[1,a)]

AFFILIATIONS

[1] Physikalisch-Technische Bundesanstalt, Bundesallee 100, 38116 Braunschweig, Germany
[2] Deutsches Zentrum für Luft- und Raumfahrt e.V. (DLR), Institut für Satellitengeodäsie und Inertialsensorik, Callinstraße 30b, 30167 Hannover, Germany

[a)] **Author to whom correspondence should be addressed:** christian.lisdat@ptb.de

ABSTRACT

We present a novel achromatic, planar, periodic mirror structure for single-beam magneto-optical trapping and demonstrate its use in the first- and second-stage cooling and trapping for different isotopes of strontium. We refer to it as a Fresnel magneto-optical trap (MOT) as the structure is inspired by Fresnel lenses. By design, it avoids many of the problems that arise for multi-color cooling using planar structures based on diffraction gratings, which have been the dominant planar structures to be used for single-beam trapping thus far. In addition to a complex design process and cost-intensive fabrication, diffraction gratings suffer from their inherent chromaticity, which causes different axial displacements of trap volumes for different wavelengths and necessitates trade-offs in their diffraction properties and achievable trap depths. In contrast, the Fresnel-reflector structure presented here is a versatile, easy-to-manufacture device that combines achromatic beam steering with the advantages of a planar architecture. It enables miniaturizing trapping systems for alkaline-earth-like atoms with multiple cooling transitions as well as multi-species trapping in the ideal tetrahedral configuration and within the same volume above the structure. Our design presents a novel approach for the miniaturization of cold-atom systems based on single-beam MOTs and enables the widespread adoption of these systems.

I. INTRODUCTION

The invention of laser cooling and trapping techniques has enabled the control and manipulation of individual quantum systems, such as ensembles of atoms, and heralded the emergence of quantum sensing based on cold atoms.[1] This field of research continues to improve measurement resolution and to revolutionize measurement capabilities in many fields, including metrology,[2–5] navigation, and inertial sensing,[6] as well as the search for new physics.[7] Optical lattice clocks[8] in frequency metrology, matter-wave interferometers[9,10] for gravimetry, and (cold-atom-based) magnetometers[11–13] are only some of the new measurement devices that are based on cold atoms. In addition, cold atoms are used in quantum computing experiments.[14–17] Due to their high accuracy, precision, and vast range of applications, cold-atom quantum sensors are transitioning from laboratory environments to field-based applications, including air- and spaceborne platforms.[18] The resulting need for (trans-)portability places stringent requirements on a sensor's size, weight, and power consumption (SWaP).[19] Miniaturizing the key components of quantum experiments to harness the capabilities of the state-of-the-art quantum sensors in field operation is thus a vital, ongoing process.[20] For neutral atoms, preparation of an ensemble for a measurement usually starts with a magneto-optical trap (MOT). A number of more compact alternatives to the traditional six-beam geometry[21] have been developed throughout the years, including the "pyramid MOT,"[22,23] "tetrahedral MOT,"[24] and "grating MOT" (gMOT).[25–27]

Grating MOTs are based on a planar, monolithic diffraction grating and thus offer the highest degree of miniaturization as well as unrestricted radial access. They have been employed in several quantum sensors using alkaline atoms already.[28–30] Here, they are well suited as alkaline atoms as they are usually cooled using a single transition with a linewidth of several megahertz and highly effective sub-Doppler cooling. However, many applications require multi-color operation with wavelengths separated by up to several hundred nanometers, including the multi-stage cool-

ing of alkaline-earth-like atoms, which is used to reach temperatures of few microkelvin,[31–33] as well as multi-species cooling and trapping, e.g., dual-species traps with alkaline atoms to produce alkaline–alkaline molecules.[34,35] Alkaline-earth-like atoms are particularly useful for many metrological and sensing applications, such as optical clocks,[8,36] due to the presence of ultranarrow optical transitions. For these applications, the inherent chromacity of diffraction gratings poses a number of challenges to cooling and trapping at two vastly different wavelengths: First, the respective trapping volumes are displaced axially, which complicates the transfer between MOT stages using different wavelengths.[37] Second, the grating needs to be specifically designed and manufactured for each atomic species or combination of species,[38] which is a costly, time-consuming, and complex process and requires micro-fabrication techniques. Finally, achieving efficient diffraction at both wavelengths may require limiting the diffraction angle θ, e.g., to $\theta < 40°$ for the 461 nm transition in Sr. This results in significantly decreased trap depths as large diffraction angles benefit the trap depth.[39,40] Additional compromises are often necessary with regard to diffraction efficiencies and polarization purity, which further impact trap dynamics.

For the bosonic isotope ^{88}Sr, two-stage cooling in a grating MOT has been demonstrated.[37,41] However, fermionic alkaline-earth atoms are often more challenging to cool and exhibit an increased sensitivity to the trap geometry,[40] because the hyperfine splitting of their energy levels and their substantially different Landé factors in the ground and excited states result in more complex cooling dynamics.[42]

The pyramid and tetrahedral MOTs, being reflective structures, are inherently achromatic and thus do not suffer from the same problems as grating MOTs for multi-color operation. They do not offer the same level of optical access and miniaturization, however: The pyramid MOT conserves the standard six-beam geometry using a number of mirror pairs that reflect the incident beam at a 90° angle.[22,23] As the trap volume lies within the pyramid, optical access is severely limited. Furthermore, this setup is relatively bulky compared to the planar chip design of grating MOTs. In the tetrahedral MOT, an incident beam is reflected by three surfaces arranged such that the incident beam and the reflected beams cross close to the tetrahedral configuration.[24] Part of the beams' overlap volume extends above the mirror structure (see Fig. 1, red dashed line). Still, optical access is severely limited since the mirrors block radial access to more than half the overlap volume. This can be compensated by pulling the mirrors apart but only at the cost of reduced laser power density or trapping volume.

Here, we present a novel type of single-beam MOT that combines unrestricted radial access and the compactness of a planar design like the grating MOT with the achromatic beam steering of reflective operation.[43] It is based on the tetrahedral mirror MOT but replaces the bulk mirrors with surface-structured Fresnel-like reflectors. This leads to a quasi-planar, achromatic, single-beam MOT with full optical access in the radial plane providing cooling in a tetrahedral geometry. In addition, the planar geometry enables the integration of further miniaturized components in a compact package, e.g., atom source, magnetic field coils, optical resonators. It further allows trapping of different atomic species at the same height over the reflector, independent of wavelength. We demonstrate two-stage trapping and cooling of ^{88}Sr atoms in the Fresnel MOT. Initially, atoms are cooled on the $^1S_0 \rightarrow {}^1P_1$ transition at a wavelength of 461 nm and a linewidth of 30.2 MHz.[44] They are then transferred to a so-called broadband MOT on the $^1S_0 \rightarrow {}^3P_1$ transition at a wavelength of 689 nm and a linewidth of 7.5 kHz,[45] reaching temperatures of 23–43 μK. We further demonstrate trapping and cooling of ^{87}Sr and ^{86}Sr atoms using the $^1S_0 \rightarrow {}^1P_1$ transition.

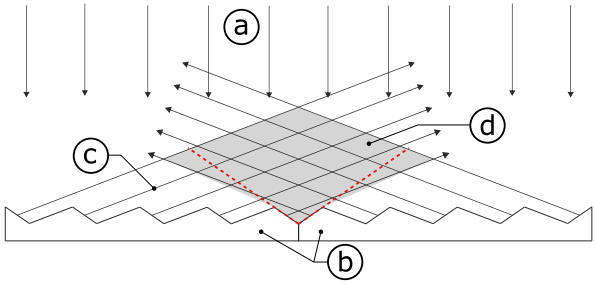

FIG. 1. Schematic of the beam propagation in the Fresnel MOT. The incident beam (a) is reflected by the Fresnel reflector (b), creating secondary beams (c). Adding a magnetic quadrupole field with its minimum within the beam overlap volume (d) leads to cooling and trapping of atoms. The red dashed lines show the equivalent mirror surfaces of a tetrahedral MOT producing an identical beam geometry. Adapted with permission from S. Bondza, "Planar structures for two-color, single-beam magneto-optical traps," Ph.D. thesis, Leibniz University Hannover, 2023.[46]

The surface structure of the Fresnel MOT is obtained when the mirror surfaces of a tetrahedral MOT are folded back onto a common plane, yielding a periodic, triangular, reflecting structure as illustrated in Fig. 1. Surfaces reflecting toward the center of the trap alternate with those reflecting outward. Ideally, the surfaces of the latter are parallel to the reflected MOT beams [(c) in Fig. 1] to prevent these beams from reaching the trapping region by multiple reflections. The height of the structure is directly related to the period and, in principle, arbitrary, as long as the period is large compared to the employed wavelength to avoid diffraction. In practice, the period should be chosen as large as conveniently possible, to minimize potential wavefront errors. In the limit of long periods, this eventually leads to the original tetrahedral MOT.

The theory of operation for the Fresnel MOT is identical to the tetrahedral MOT, covered extensively by Vangeleyn *et al.*[24,39] A stable optical molasses is produced with a set of beams with a balanced radiation pressure,

$$\sum_{n=1}^{N_{tot}} I_n \vec{k_n} = 0, \tag{1}$$

where I_n and $\vec{k_n}$ are the intensity and wave vector of beam n, respectively, and N_{tot} is the total number of beams. In the radial plane, given a radially symmetric formation of secondary beams, this condition is fulfilled when illuminating the structure with a flat-top intensity profile. Axially, the secondary beam intensity can be controlled via the reflectivity R of the Fresnel reflector. For N secondary beams, a balanced radiation pressure is achieved for a mirror inclination with respect to the incident beam of

$$\phi = \frac{1}{2} \arccos \frac{1}{NR}. \tag{2}$$

The angle between the incident and secondary beams is then given as $\theta = 2\phi$, which corresponds to the convention of the diffraction angle given for grating MOTs. The minimum number of secondary beams for three-dimensional trapping is $N = 3$, which also leads to the largest possible beam overlap volume. In this case, a mirror inclination of up to $\phi = 35.26°$, corresponding to the tetrahedral configuration, with a reflectivity of $R = 1$ of the mirror surfaces can be chosen. Choosing an angle requires a trade-off between the size of the capture volume, which is largest for small inclination angles, and ideal trapping and cooling, which is achieved for the tetrahedral geometry. As the increase in trap volume is mainly due to its elongation and ideal trapping and cooling forces are vital to achieve a large number of atoms at low final temperatures,[43] we prioritize the latter. However, analyzing the trapping and cooling dynamics and resulting ideal geometries for different atoms is complex and research is ongoing.[47,48]

The main advantage of the Fresnel MOT over the standard tetrahedral mirror MOT is the possibility for a much more compact, quasi-planar design with radial access as the grating MOT offers. In addition, strong trapping and radial cooling close to the tetrahedral configuration is maintained independent of wavelength. Fresnel MOTs thus lend themselves for use in miniaturized vacuum systems of a few cubic centimeter volume. Apart from light, another critical aspect of MOTs is the generation of sufficiently strong magnetic field, which is often generated by a pair of coils in or near the anti-Helmholtz configuration. In order to minimize their SWaP, placing them as close as possible to the trap volume is mandatory, which is supported by our Fresnel MOT approach. Especially for alkaline-earth atom MOTs, which require a larger magnetic field gradient compared to alkaline atoms, this can lead to designs that forego the common water cooling of the field coils.

II. EXPERIMENT

A prototype of the Fresnel MOT was manufactured from oxygen-free high-conductivity copper. This material is well-suited for this purpose, as a mirror-finish surface can be produced by milling processes alone, without subsequent polishing. Three individual 120° circle segments were machined that, put together, result in a 25.4 mm diameter reflector, which is depicted in Fig. 2. The copper substrates where sputter-coated with a 100 nm layer of aluminum that serves as a highly reflective surface in the visible wavelength range. The reflectivity of aluminum in the visible spectrum is about 90%. This determined the mirror inclination according to Eq. (2) to 34°, yielding an angle between the incident and secondary beams of $\theta = 68°$. The assembled device features a triangular hole in the center that can potentially be used to load atoms into the trap as shown in a study by Sitaram *et al.*[49] Polarization conservation of the reflector was measured with a polarimeter and found to be ≈95 %. The root-mean-square surface roughness was measured with white light interferometry, yielding 7 nm.

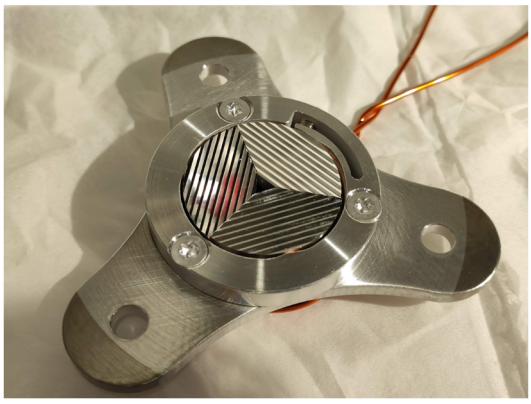

FIG. 2. Photograph of the Fresnel reflector in a 25.4 mm flexure mount.

The test setup used to characterize the chip has been presented in detail in a previous publication:[37] A bi-chromatic laser beam red-detuned with respect to the $^1S_0 \rightarrow {}^1P_1$ transition of strontium at 461 nm and the $^1S_0 \rightarrow {}^3P_1$ transition at 689 nm is circularly polarized and shaped to a flat-top intensity profile with 18 mm in diameter.

For the first cooling stage, up to 43 mW of optical power at 461 nm is incident on the Fresnel reflector, yielding $\frac{I}{I_{sat}} = 0.4$, where I denotes the laser intensity of the incident beam and $I_{sat} = 43\ \mathrm{mW/cm^2}$, the saturation intensity of the transition. A set of in-vacuum anti-Helmholtz coils generate a magnetic field gradient of up to 7 mT/cm along the incident beam axis. The MOT is loaded from an atomic beam parallel to the Fresnel reflector surface, provided by an atomic oven. This oven is typically operated at temperatures ranging between 350 and 400 °C. Some of the atoms are pre-slowed below the MOT capture velocity by a counterpropagating deceleration beam, red-detuned by about 200 MHz.

For the second cooling stage, up to 15 mW of power is available corresponding to a saturation parameter of $s \approx 1000$. In this stage, the magnetic field gradient is reduced to about 0.3 mT/cm. To allow axial positioning control of the trapping center, additional magnetic field coils enable the application of a bias field that offsets the quadrupole magnetic field minimum. As the $^1S_0 \rightarrow {}^1P_1$ transition is not a closed transition, atoms can escape the cooling cycle by decay to either the $^3P_0$ or $^3P_2$ dark state via the intermediate $^1D_2$ state as illustrated in Fig. 3. To overcome this issue, we employ a repumping scheme using 679 and 707 nm.[50] The repump beams propagate in parallel to the reflector and are retroreflected. To carry out our characterization measurements, laser-induced fluorescence on the $^1S_0 \rightarrow {}^1P_1$ transition is used. The fluorescence signal is collected by a large numerical aperture lens and imaged either on a CMOS camera with which we carry out atomic temperature measurements or a photomultiplier tube (PMT) to measure MOT lifetimes.

After the conclusion of the experiments, the Fresnel-reflector was removed, and upon visual inspection, no coating of strontium was observed. A potential coating of the Fresnel-reflector with strontium can further be prevented by the use of a loading geometry along the axial direction as presented in a study by Sitaram *et al.*[49]

III. RESULTS

We typically trap $5 \cdot 10^6$–$8 \cdot 10^6$ ^{88}Sr atoms in the first MOT stage operated on the 461 nm $^1S_0 \rightarrow {}^1P_1$ transition. We evaluate the MOT regarding lifetime and temperature. The temperature is evaluated with the time of flight (TOF) method as a function of intensity of the incident MOT beam. The atoms are initially loaded into the Fresnel MOT with MOT beams at $\frac{I}{I_{sat}} = 0.4$. The intensity is then decreased to the target intensity. Once the atoms are thermalized, the

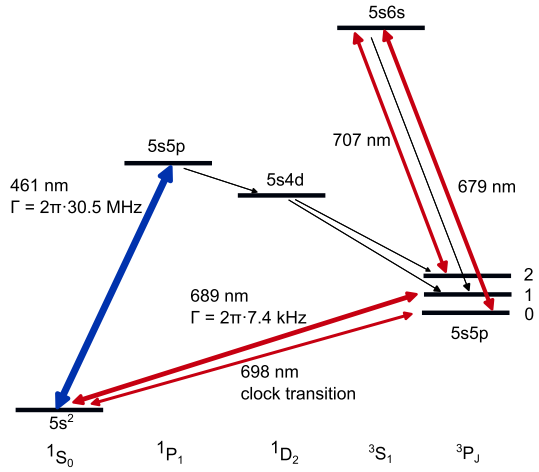

FIG. 3. Partial energy level diagram of ^{88}Sr with cooling transitions and their linewidths, the clock transition, as well as repumper transitions.

trapping light is switched off and the atomic cloud expands freely. The diameter of the atom cloud σ is observed at time t, and the temperature is extracted from $\sigma^2(t) = \sigma_0^2 + (k_B T/M) \times t^2$. Here, σ_0 is the initial size of the atomic cloud and $k_B T/M$ is their thermal energy per atomic mass. The images of the expanding cloud are recorded with fluorescence imaging with an illumination time of 100 μs.

The dependency of temperature on laser intensity is depicted in Fig. 4. The lowest temperatures are achieved for a saturation parameter of $\frac{I}{I_{sat}} = 0.06$, with 3.87 (0.10) mK in the axial direction and 4.28 (0.12) mK in the radial direction, respectively. For smaller intensities, the atom number becomes too small for temperature measurements due to a high loss rate. These results are comparable with temperatures reached in strontium grating MOTs,[37,49] and

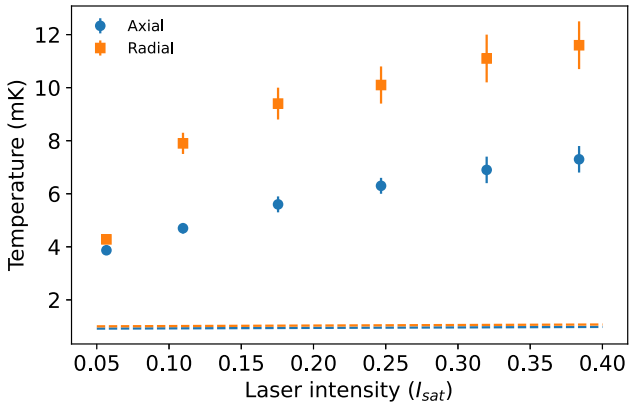

FIG. 4. Axial (blue) and radial (orange) temperatures in the first stage MOT as a function of incident laser intensity with $dB/dz = 7$ mT/cm. Temperature is measured with the TOF method. The dashed lines indicate the theoretical Doppler limit for both axial and radial directions. Adapted with permission from S. Bondza, "Planar structures for two-color, single-beam magneto-optical traps," Ph.D. thesis, Leibniz University Hannover, 2023.[46]

the atoms are sufficiently cold to be transferred to the next cooling stage.

The Doppler limit in the radial and axial directions as a function of the angle θ is given as $T_{rad} = \frac{T_D}{6} \cdot \left(3 + \frac{1}{\cos(\theta)}\right)$ and $T_{ax} = \frac{T_D}{6} \cdot \left(3 + \frac{1}{\sin^2(\theta/2)}\right)$, respectively.[51] The ratio of the radial to axial temperature agrees with the expected value of 1.1 within one standard deviation for the lowest achieved temperatures. However, the measured temperatures lie above the theoretical Doppler limit with an increase much stronger than expected from the Doppler limit. This effect is commonly observed in alkaline-earth atoms[52–55] and has been linked to an additional heating mechanism originating from transverse spatial intensity fluctuations.[56] At low velocities, cooling is described by a frictional force and an additional constant force resulting from intensity fluctuations. Both forces are intensity dependent; the effect thus increases with increasing intensity. The possible sources of spatial intensity fluctuations in the Fresnel MOT originate from the beam profile, imperfect edges of neighboring surfaces of the Fresnel structure, imperfections in the coating, and slight misalignment of the beam. None of these factors are fundamental limitations, and we expect that the performance of the Fresnel MOT can be improved by addressing these issues. In addition, spatial intensity fluctuations may also result from near-field diffractive effects originating from light passing a hard edge, which remains to be investigated.

We further analyzed the first cooling stage with respect to lifetime. The lifetime τ can be determined from a loading curve with $N_{atoms}(t) = r\tau(1 - e^{-t/\tau})$, where r is the loading rate and N_{atoms} is the atom number.[49] We found that the lifetime shows a dependency on laser intensity as well as magnetic field gradient as presented in Fig. 5.

We observe the lifetime of the atoms in the MOT to decrease with increasing intensity. One possible explanation lies in the strong increase in temperature. Fast atoms are more likely to be able to escape the trap while in a dark state before being able to be repumped, resulting in a loss channel. We observed that decreasing the power in the repumping beams decreases the atom number,

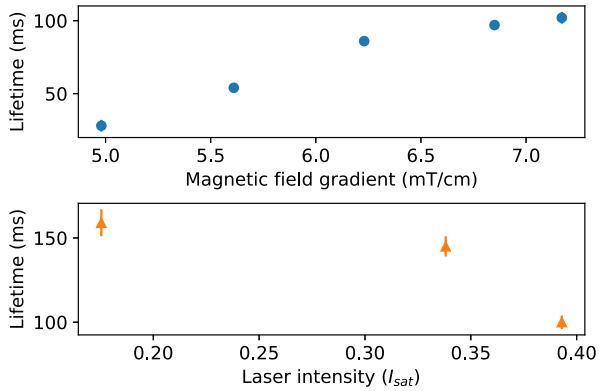

FIG. 5. Lifetime in the $^1S_0 \rightarrow {}^1P_1$ MOT as a function of magnetic field gradient with $\frac{I}{I_{sat}} = 0.4$ and laser intensity with $dB/dz = 7$ mT/cm. The vacuum pressure is $5 \cdot 10^{-9}$ mbar corresponding to a background-gas-collision limited lifetime of 660 ms.

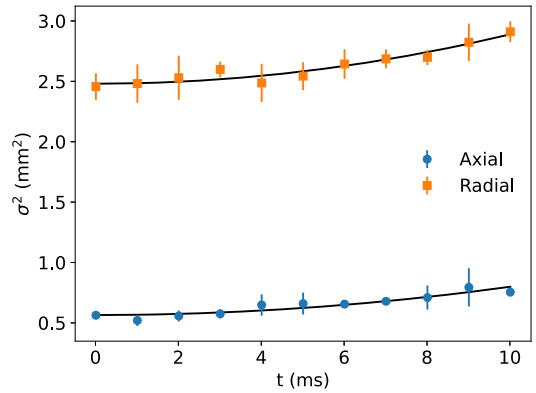

FIG. 6. Expansion of the atomic cloud in the axial (blue) and radial (orange) directions with time after the broadband MOT on the $^1S_0 \rightarrow {}^3P_1$ transition. The fit yields $T_{ax} = 23(3)\ \mu$K and $T_{rad} = 43(4)\ \mu$K.

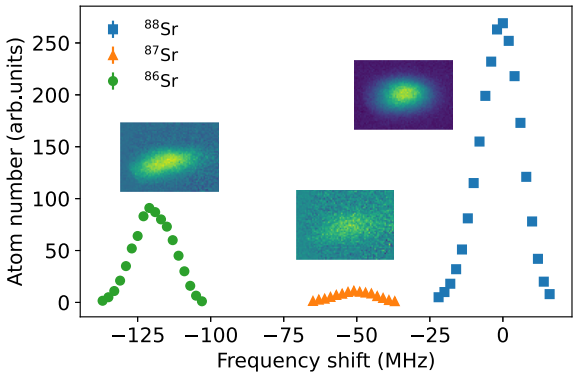

FIG. 7. Atom number as a function of frequency detuning for ^{88}Sr, ^{87}Sr, and ^{86}Sr. The insets show the fluorescence images for the atom clouds. For ^{86}Sr and ^{87}Sr, multiple images are averaged and the averaged background subtracted to obtain an improved signal to noise. Furthermore, the exposure time is increased from 100 to 300 μs. Adapted with permission from S. Bondza, "Planar structures for two-color, single-beam magneto-optical traps," Ph.D. thesis, Leibniz University Hannover, 2023.[46]

which supports this explanation. The lifetime increases with increasing magnetic field gradient as previously observed in the grating MOT as well.[37,49] We measured a maximal lifetime of $\tau_{tot} = 160$ ms at a vacuum pressure of $5 \cdot 10^{-9}$ mbar at a laser intensity $\frac{I}{I_{sat}} = 0.18$. At $5 \cdot 10^{-9}$ mbar, background gas collisions limit the MOT lifetime to about 660 ms.[57] In our setup, outgassing from the strontium oven limits the vacuum pressure.

We transfer the pre-cooled ^{88}Sr atoms to a broadband MOT operated on the $^1S_0 \rightarrow {}^3P_1$ transition at 689 nm where the laser was artificially broadened to about 1 MHz. This procedure is common and improves transfer efficiency as a temperature in the milli-kelvin range corresponds to a Doppler shift on the order of megahertz.[31] We achieve a transfer efficiency of 50%, comparable to typical transfer efficiencies in the six-beam geometry. Here, the atoms were further cooled to a temperature of $(23 \pm 3)\ \mu$K in the axial direction and $(43 \pm 4)\ \mu$K in the radial direction, as shown in Fig. 6. This result presents a first demonstration of multi-color cooling with the novel structure. As a next step, the atoms can be loaded into a dipole trap for further cooling. The trap depths for optical lattices typically reach few hundred recoil energies corresponding to tens of microkelvins.[58] To optimize the transfer efficiency to a dipole trap, the atoms are commonly further pre-cooled on the $^1S_0 \rightarrow {}^3P_1$ transition in a so-called single-frequency MOT where narrow-line cooling laser is used. An unmodulated, narrow-line, single-frequency grating MOT with a similar geometry has already been demonstrated for strontium, reaching temperatures below 10 μK.[37,41]

Apart from ^{88}Sr, we also trapped and cooled ^{86}Sr as well as the fermionic isotope ^{87}Sr on the $^1S_0 \rightarrow {}^1P_1$ transition. We observe an axial shift between the bosonic and fermionic MOTs, which is consistent with a theory of the trapping dynamics[40] and previous observations by other groups.[41]

To improve the atom number for the ^{86}Sr and ^{87}Sr MOTs, we increase the temperature of the thermal atom source to 400 °C, thus generating a higher atom flux. Figure 7 shows the relative atom number as a function of detuning of the cooling laser for ^{86}Sr, ^{87}Sr, and ^{88}Sr, where 0 MHz detuning is chosen as the frequency yielding the maximum atom number for ^{88}Sr. The frequency shifts for ^{86}Sr. and ^{87}Sr. correspond to the isotope shifts of the $^1S_0 \rightarrow {}^1P_1$ transition.[59]

While ^{86}Sr and ^{87}Sr have a similar abundance, we trap about four times as much ^{86}Sr as ^{87}Sr. One possible reason lies in the loss channel is insufficient repumping for fast atoms impacting fermionic strontium more severely, as the repumping lasers need to be frequency modulated to cover all Zeeman sublevels, which reduces the saturation parameter. To increase the atom number for ^{87}Sr and the signal to noise ratio, more efficient loading geometries can be employed, including a Zeeman slower.

IV. CONCLUSION

We have demonstrated two-stage laser cooling of bosonic ^{88}Sr to microkelvin temperatures and trapping of ^{86}Sr and fermionic ^{87}Sr in the first MOT stage with a novel, quasi-planar, achromatic reflector in a single-beam geometry. The Fresnel reflector is a low-cost, easy-to-manufacture device without the need for microfabrication technologies. It further combines the advantages of the grating MOT offering unrestricted radial access and a high level of miniaturization with the achromatic beam path of the tetrahedral MOT. This enables trapping within a fixed volume in an ideal tetrahedral geometry independent of wavelengths, thus allowing for optimized trap depths, which is critical, in particular, for fermionic alkaline-earth-like isotopes. As a result, it promises new possibilities for robust, multi-color cooling of one or multiple atomic species.We expect that the performance of the Fresnel MOT can be further improved by addressing sources of spatial intensity fluctuations, such as uneven reflectivity of the coating and imperfect edges of neighboring surfaces, employing differential pumping to reduce the vacuum pressure, and a more sophisticated loading scheme, increasing the atom number and reducing the background fluorescence. Our work is an important step in the widespread adoption of single-beam MOT designs based on planar structures for quantum sensors aiding the essential reduction in their SWaP.

ACKNOWLEDGEMENT

We thank Stephan Metschke and his group for the manufacturing of the Fresnel structure and Andre Felgner for the characterization of its surface. We further thank Sören Dörscher for careful reading of the manuscript and helpful discussion. This work was financially supported by the State of Lower-Saxony through the VW Vorab. We further acknowledge the support by the Deutsche Forschungsgemeinschaft (DFG, German Research Foundation) under Germany's Excellence Strategy—EXC-2123 QuantumFrontiers—Project No. 390837967.

AUTHOR DECLARATIONS

Conflict of Interest

S.A.B., T.L., and C.L. are inventors of Patent DE: 10 2020 102 222.0. PTB holds the rights to this patent.

Author Contributions

S. A. Bondza: Data curation (lead); Formal analysis (lead); Investigation (lead); Methodology (equal); Visualization (lead); Writing – original draft (lead); Writing – review & editing (lead). **T. Leopold**: Conceptualization (supporting); Methodology (supporting); Supervision (supporting). **R. Schwarz**: Investigation (supporting); Writing – original draft (supporting); Writing – review & editing (supporting). **C. Lisdat**: Conceptualization (lead); Methodology (supporting); Project administration (equal); Resources (equal); Supervision (lead); Visualization (supporting); Writing – original draft (supporting); Writing – review & editing (supporting).

DATA AVAILABILITY

The data that support the findings of this study are available from the corresponding author upon reasonable request.

REFERENCES

[1] C. L. Degen, F. Reinhard, and P. Cappellaro, "Quantum sensing," Rev. Mod. Phys. **89**, 035002 (2017).
[2] S. Eckel, D. S. Barker, J. A. Fedchak, N. N. Klimov, E. Norrgard, J. Scherschligt, C. Makrides, and E. Tiesinga, "Challenges to miniaturizing cold atom technology for deployable vacuum metrology," Metrologia **55**, S182–S193 (2018).
[3] W. F. McGrew, X. Zhang, H. Leopardi, R. J. Fasano, D. Nicolodi, K. Beloy, J. Yao, J. A. Sherman, S. A. Schäffer, J. Savory, R. C. Brown, S. Römisch, C. W. Oates, T. E. Parker, T. M. Fortier, and A. D. Ludlow, "Towards the optical second: Verifying optical clocks at the SI limit," Optica **6**, 448–454 (2019).
[4] F. Riehle, "Towards a redefinition of the second based on optical atomic clocks," C. R. Phys. **16**, 506–515 (2015), part of Special Issue: The measurement of time/La mesure du temps.
[5] J. Scherschligt, J. A. Fedchak, Z. Ahmed, D. S. Barker, K. Douglass, S. Eckel, E. Hanson, J. Hendricks, N. Klimov, T. Purdy, J. Ricker, R. Singh, and J. Stone, "Review article: Quantum-based vacuum metrology at the national institute of standards and technology," J. Vac. Sci. Technol., A **36**, 040801 (2018).
[6] C. L. Garrido Alzar, "Compact chip-scale guided cold atom gyrometers for inertial navigation: Enabling technologies and design study," AVS Quantum Sci. **1**, 014702 (2019).
[7] M. Safronova, D. Budker, D. DeMille, D. F. J. Kimball, A. Derevianko, and C. W. Clark, "Search for new physics with atoms and molecules," Rev. Mod. Phys. **90**, 025008 (2018).
[8] A. D. Ludlow, M. M. Boyd, J. Ye, E. Peik, and P. O. Schmidt, "Optical atomic clocks," Rev. Mod. Phys. **87**, 637–701 (2015).
[9] A. Peters, K. Y. Chung, and S. Chu, "Measurement of gravitational acceleration by dropping atoms," Nature **400**, 849–852 (1999).
[10] M. Kasevich and S. Chu, "Measurement of the gravitational acceleration of an atom with a light-pulse atom interferometer," Appl. Phys. B **54**, 321–332 (1992).
[11] M. Vengalattore, J. M. Higbie, S. R. Leslie, J. Guzman, L. E. Sadler, and D. M. Stamper-Kurn, "High-resolution magnetometry with a spinor Bose–Einstein condensate," Phys. Rev. Lett. **98**, 200801 (2007).
[12] C. F. Ockeloen, R. Schmied, M. F. Riedel, and P. Treutlein, "Quantum metrology with a scanning probe atom interferometer," Phys. Rev. Lett. **111**, 143001 (2013).
[13] S. Wildermuth, S. Hofferberth, I. Lesanovsky, E. Haller, L. M. Andersson, S. Groth, I. Bar-Joseph, P. Krüger, and J. Schmiedmayer, "Bose–Einstein condensates: Microscopic magnetic-field imaging," Nature **435**, 440 (2005).
[14] A. Kaufman, B. Lester, M. Foss-Feig, M. L. Wall, A. M. Rey, and C. Regal, "Entangling two transportable neutral atoms via local spin exchange," Nature **527**, 208–211 (2015).
[15] C. J. Picken, R. Legaie, K. McDonnell, and J. D. Pritchard, "Entanglement of neutral-atom qubits with long ground-Rydberg coherence times," Quantum Sci. Technol. **4**, 015011 (2018).
[16] M. Saffman, "Quantum computing with atomic qubits and Rydberg interactions: Progress and challenges," J. Phys. B: At., Mol. Opt. Phys. **49**, 202001 (2016).
[17] L. Henriet, L. Beguin, A. Signoles, T. Lahaye, A. Browaeys, G.-O. Reymond, and C. Jurczak, "Quantum computing with neutral atoms," Quantum **4**, 327 (2020).
[18] G. Tino, L. Cacciapuoti, K. Bongs, C. J. Bordé, P. Bouyer, H. Dittus, W. Ertmer, A. Görlitz, M. Inguscio, A. Landragin, P. Lemonde, C. Lämmerzahl, A. Peters, E. Rasel, J. Reichel, C. Salomon, S. Schiller, W. Schleich, K. Sengstock, U. Sterr, and M. Wilkens, "Atom interferometers and optical atomic clocks: New quantum sensors for fundamental physics experiments in space," Nucl. Phys. B, Proc. Suppl. **166**, 159–165 (2007).
[19] K. Bongs, M. Holynski, J. Vovrosh, P. Bouyer, G. Condon, E. Rasel, C. Schubert, W. Schleich, and A. Roura, "Taking atom interferometric quantum sensors from the laboratory to real-world applications," Nat. Rev. Phys. **1**, 731–739 (2019).
[20] J. P. McGilligan, K. Gallacher, P. F. Griffin, D. J. Paul, A. S. Arnold, and E. Riis, "Micro-fabricated components for cold atom sensors," Rev. Sci. Instrum. **93**, 091101 (2022).
[21] E. L. Raab, M. Prentiss, A. Cable, S. Chu, and D. E. Pritchard, "Trapping of neutral sodium atoms with radiation pressure," Phys. Rev. Lett. **59**, 2631–2634 (1987).
[22] K. I. Lee, J. A. Kim, H. R. Noh, and W. Jhe, "Single-beam atom trap in a pyramidal and conical hollow mirror," Opt. Lett. **21**, 1177–1179 (1996).
[23] W. Bowden, R. Hobson, I. R. Hill, A. Vianello, M. Schioppo, A. Silva, H. S. Margolis, P. E. G. Baird, and P. Gill, "A pyramid MOT with integrated optical cavities as a cold atom platform for an optical lattice clock," Sci. Rep. **9**, 11704 (2019).
[24] M. Vangeleyn, P. F. Griffin, E. Riis, and A. S. Arnold, "Single-laser, one beam, tetrahedral magneto-optical trap," Opt. Express **17**, 13601–13608 (2009).
[25] J. P. McGilligan, P. F. Griffin, E. Riis, and A. S. Arnold, "Diffraction-grating characterization for cold-atom experiments," J. Opt. Soc. Am. B **33**, 1271–1277 (2016).
[26] J. P. McGilligan, P. F. Griffin, R. Elvin, S. J. Ingleby, E. Riis, and A. S. Arnold, "Grating chips for quantum technologies," Sci. Rep. **7**, 384 (2017).
[27] C. C. Nshii, M. Vangeleyn, J. P. Cotter, P. F. Griffin, E. A. Hinds, C. N. Ironside, P. See, A. G. Sinclair, E. Riis, and A. S. Arnold, "A surface-patterned chip as a strong source of ultracold atoms for quantum technologies," Nat. Nanotechnol. **8**, 321–324 (2013).
[28] R. Elvin, G. W. Hoth, M. Wright, B. Lewis, J. P. McGilligan, A. S. Arnold, P. F. Griffin, and E. Riis, "Cold-atom clock based on a diffractive optic," Opt. Express **27**, 38359–38366 (2019).
[29] D. S. Barker, E. B. Norrgard, N. N. Klimov, J. A. Fedchak, J. Scherschligt, and S. Eckel, "Single-beam Zeeman slower and magneto-optical trap using a nanofabricated grating," Phys. Rev. Appl. **11**, 064023 (2019).
[30] J. Lee, R. Ding, J. Christensen, R. R. Rosenthal, A. Ison, D. P. Gillund, D. Bossert, K. H. Fuerschbach, W. Kindel, P. S. Finnegan, J. R. Wendt, M. Gehl, A. Kodigala, H. McGuinness, C. A. Walker, S. A. Kemme, A. Lentine, G. Biedermann, and P. D.

D. Schwindt, "A compact cold-atom interferometer with a high data-rate grating magneto-optical trap and a photonic-integrated-circuit-compatible laser system," Nat. Communcations **13**, 5131 (2022).
[31]H. Katori, T. Ido, Y. Isoya, and M. Kuwata-Gonokami, "Magneto-optical trapping and cooling of strontium atoms down to the photon recoil temperature," Phys. Rev. Lett. **82**, 1116–1119 (1999).
[32]T. Kuwamoto, K. Honda, Y. Takahashi, and T. Yabuzaki, "Magneto-optical trapping of Yb atoms using an intercombination transition," Phys. Rev. A **60**, R745–R748 (1999).
[33]S. Dörscher, A. Thobe, B. Hundt, A. Kochanke, R. Le Targat, P. Windpassinger, C. Becker, and K. Sengstock, "Creation of quantum-degenerate gases of ytterbium in a compact 2D-/3D-magneto-optical trap setup," Rev. Sci. Instrum. **84**, 043109 (2013).
[34]S. D. Kraft, P. Staanum, J. Lange, L. Vogel, R. Wester, and M. Weidemüller, "Formation of ultracold LiCs molecules," J. Phys. B: At., Mol. Opt. Phys. **39**, S993–S1000 (2006).
[35]J. P. Shaffer, W. Chalupczak, and N. P. Bigelow, "Photoassociative ionization of heteronuclear molecules in a novel two-species magneto-optical trap," Phys. Rev. Lett. **82**, 1124–1127 (1999).
[36]L. Hu, N. Poli, L. Salvi, and G. M. Tino, "Atom interferometry with the Sr optical clock transition," Phys. Rev. Lett. **119**, 263601 (2017).
[37]S. Bondza, C. Lisdat, S. Kroker, and T. Leopold, "Two-color grating magneto-optical trap for narrow-line laser cooling," Phys. Rev. Appl. **17**, 044002 (2022).
[38]O. S. Burrow, R. J. Fasano, W. Brand, M. W. Wright, W. Li, A. D. Ludlow, E. Riis, P. F. Griffin, and A. S. Arnold, "Optimal binary gratings for multi-wavelength magneto-optical traps," Opt. Express **31**, 40871–40880 (2023).
[39]M. Vangeleyn, "Atom trapping in non-trivial geometries for micro-fabrication applications," Ph.D. thesis, University of Strathclyde, 2011.
[40]D. S. Barker, P. K. Elgee, A. Sitaram, E. B. Norrgard, N. N. Klimov, G. K. Campbell, and S. Eckel, "Grating magneto-optical traps with complicated level structures," New J. Phys. **25**, 103046 (2023).
[41]P. K. Elgee, "Grating magneto-optical trap for strontium," Ph.D. thesis, University of Maryland, 2022.
[42]T. Mukaiyama, H. Katori, T. Ido, Y. Li, and M. Kuwata-Gonokami, "Recoil-limited laser cooling of Sr atoms near the Fermi temperature," Phys. Rev. Lett. **90**, 113002 (2003).
[43]S. Bondza, T. Leopold, and C. Lisdat, "Atomfalle und verfahren zum kühlen oder einfangen von atomen," German patent DE102020102222B4 (14 July 2022).
[44]T. L. Nicholson, S. L. Campbell, R. B. Hutson, G. E. Marti, B. J. Bloom, R. L. McNally, W. Zhang, M. D. Barrett, M. S. Safronova, G. F. Strouse, W. L. Tew, and J. Ye, "Systematic evaluation of an atomic clock at 2×10^{-18} total uncertainty," Nat. Commun. **6**, 6896 (2015).
[45]M. Yasuda, T. Kishimoto, M. Takamoto, and H. Katori, "Photoassociation spectroscopy of ^{88}Sr: Reconstruction of the wave function near the last node," Phys. Rev. A **73**, 011403(R) (2006).
[46]S. Bondza, "Planar structures for two-color, single-beam magneto-optical traps," Ph.D. thesis, Leibniz University Hannover, 2023.
[47]S. Seo, J. H. Lee, S.-B. Lee, S. E. Park, M. H. Seo, J. Park, T. Y. Kwon, and H.-G. Hong, "Maximized atom number for a grating magneto-optical trap via machine-learning assisted parameter optimization," Opt. Express **29**, 35623–35639 (2021).
[48]O. S. Burrow, R. J. Fasano, W. Brand, M. W. Wright, W. Li, A. D. Ludlow, E. Riis, P. F. Griffin, and A. S. Arnold, "Optimal binary gratings for multi-wavelength magneto-optical traps," Opt. Express **31**, 40871–40880 (2023).
[49]A. Sitaram, P. K. Elgee, G. K. Campbell, N. N. Klimov, S. Eckel, and D. S. Barker, "Confinement of an alkaline-earth element in a grating magneto-optical trap," Rev. Sci. Instrum. **91**, 103202 (2020).
[50]S. Falke, H. Schnatz, J. S. R. V. Winfred, T. Middelmann, S. Vogt, S. Weyers, B. Lipphardt, G. Grosche, F. Riehle, U. Sterr, and C. Lisdat, "The ^{87}Sr optical frequency standard at PTB," Metrologia **48**, 399–407 (2011).
[51]J. P. McGilligan, P. F. Griffin, E. Riis, and A. S. Arnold, "Phase-space properties of magneto-optical traps utilising micro-fabricated gratings," Opt. Express **23**, 8948–8959 (2015).
[52]X. Xu, T. Loftus, M. J. Smith, J. L. Hall, A. Gallagher, and J. Ye, "Dynamics in a two-level atom magneto-optical trap," Phys. Rev. A **66**, 011401(R) (2002).
[53]X. Xu, T. H. Loftus, J. L. Hall, A. Gallagher, and J. Ye, "Cooling and trapping of atomic strontium," J. Opt. Soc. Am. B **20**, 968–976 (2003).
[54]F. Y. Loo, A. Brusch, S. Sauge, M. Allegrini, E. Arimondo, N. Andersen, and J. W. Thomsen, "Investigations of a two-level atom in a magneto-optical trap using magnesium," J. Opt. B: Quantum Semiclass. Opt. **6**, 81 (2004).
[55]C. W. Oates, F. Bondu, R. W. Fox, and L. Hollberg, "A diode-laser optical frequency standard based on laser-cooled Ca atoms: Sub-kilohertz spectroscopy by optical shelving detection," Eur. Phys. J. D **7**, 449–460 (1999).
[56]T. Chanelière, J.-L. Meunier, R. Kaiser, C. Miniatura, and D. Wilkowski, "Extra-heating mechanism in Doppler cooling experiments," J. Opt. Soc. Am. B **22**, 1819–1828 (2005).
[57]S. B. Nagel, C. E. Simien, S. Laha, P. Gupta, V. S. Ashoka, and T. C. Killian, "Magnetic trapping of metastable $^3P_2$ atomic strontium," Phys. Rev. A **67**, 011401 (2003).
[58]R. Hobson, W. Bowden, A. Vianello, A. Silva, C. F. A. Baynham, H. S. Margolis, P. E. G. Baird, P. Gill, and I. R. Hill, "A strontium optical lattice clock with 1×10^{-17} uncertainty and measurement of its absolute frequency," Metrologia **57**, 065026 (2020).
[59]C. J. Lorenzen, K. Niemax, and L. R. Pendrill, "Isotope shifts of energy levels in the naturally abundant isotopes of strontium and calcium," Phys. Rev. A **28**, 2051–2058 (1983).